

# Directed flow of identified hadrons in Au+Au collisions with the STAR experiment at RHIC

Kishora Nayak (for the STAR Collaboration)

Key Laboratory of Quark & Lepton Physics (MOE) and Institute of Particle Physics,  
Central China Normal University, Wuhan 430079, China,  
k.nayak1234@gmail.com

1        **Abstract.** Rapidity-odd component of the directed flow ( $v_1$ ) is consid-  
2        ered to be sensitive to the early collision dynamics and the equation  
3        of state (EoS) of the QCD matter formed in heavy-ion collisions. Hy-  
4        drodynamic models predict that the double sign change of  $v_1$  slope at  
5        mid-rapidity ( $dv_1/dy$ ) of net-baryon is a signature of the first-order phase  
6        transition. The STAR experiment at RHIC shows that the collision en-  
7        ergy dependences of  $dv_1/dy$  of net-proton and net- $\Lambda$  reach a minimum at  
8         $\sqrt{s_{NN}} = 14.5$  GeV, implying the possible softening of the EoS. We fur-  
9        ther explore such observations with new measurements. A comprehensive  
10       transverse momentum ( $p_T$ ) dependent  $v_1$  measurement of identified light  
11       hadrons ( $\pi^+$ ,  $\pi^-$ ,  $K^+$ ,  $K^-$ ,  $p$ ,  $\bar{p}$ ) enables us to test the constituent quark  
12       number scaling and provides a better understanding of the coalescence  
13       mechanism of particle production. In this proceeding, new results of  $p_T$   
14       and rapidity dependent  $v_1$  for identified hadrons in Au+Au collisions at  
15        $\sqrt{s_{NN}} = 19.6, 27,$  and  $54.4$  GeV are presented. These results are com-  
16       pared to AMPT model calculations.

17        **Keywords:** Directed flow, QCD phase structure, Quark-gluon plasma

## 18    1    Introduction

19       The beam energy scan program of the STAR experiment at RHIC aims to un-  
20       derstand the QCD phase diagram of strongly interacting matter produced by  
21       the ultra-relativistic heavy-ion collisions [1]. The first-order coefficient of Fourier  
22       expansion of emitted particles in the momentum space is called directed flow  
23       ( $v_1$ ). The rapidity-odd,  $v_1(y) = -v_1(-y)$ , component of the directed flow is a  
24       sensitive probe of the bulk to study the collective phenomenon in the early stage  
25       of the collisions dynamics. A first-order phase transition is predicted by various  
26       transport and hydrodynamics models [2, 3]. The model calculations show a sign  
27       change in the  $v_1$ -slope ( $dv_1/dy$ ) as function of beam energy for baryons. The  
28       QCD lattice calculations also predict the first-order phase transition [4].

29       The number of constituent quark (NCQ) of elliptic flow ( $v_2$ ) of identified  
30       hadrons in BES energies suggests that the flow is developed in the early stage of  
31       collisions and also the hadrons are formed via quarks coalescence [5–7]. However,  
32       at lower energies hadronic matter dominates. For the first time a comprehensive

33  $p_T$  dependent study of identified hadrons directed flow at different energies are  
 34 reported here. The rapidity dependence study in BES energies has been pub-  
 35 lished by the STAR Collaboration [8].

## 36 2 Directed flow of identified hadrons

37 The  $p_T$  dependent  $v_1$  of  $\pi^\pm$ ,  $K^\pm$ ,  $p$  and  $\bar{p}$  in the rapidity region  $0.5 < |y| < 1$  for  
 38 10-40% centrality in Au+Au collisions at  $\sqrt{s_{NN}} = 27$  GeV along with different  
 39 tunes of AMPT model calculations are shown in Fig. 1. For all the measured  
 40 hadrons (except proton), the  $v_1$  values are found to be negative (anti-flow) for  
 41  $p_T$  below 2.5 GeV/c (1.8 GeV/c for proton). The negative  $v_1$  at low  $p_T$  region  
 42 suggests that the produced bulk matter and formed hadrons move opposite to  
 43 each other [9–12]. However, one can not rule out the effect of shadowing in the  
 44 low  $p_T$  region [13]. The AMPT calculations are also compared with the corre-  
 45 sponding hadrons. The AMPT-Default configuration qualitatively well describes  
 46 the hadrons ( $\pi^\pm$ ,  $K^+$ ,  $p$ ) formed by quarks (anti-quarks) contributed from both  
 47 transported and produced quarks [14]. The produced hadrons such as  $K^-$ ,  $\bar{p}$  are  
 48 formed from the produced quark and anti-quark. These hadrons are qualitatively  
 49 well described by AMPT-SM with hadronic interaction time,  $t_{max} = 0.4$  and 30  
 50 fm/c.

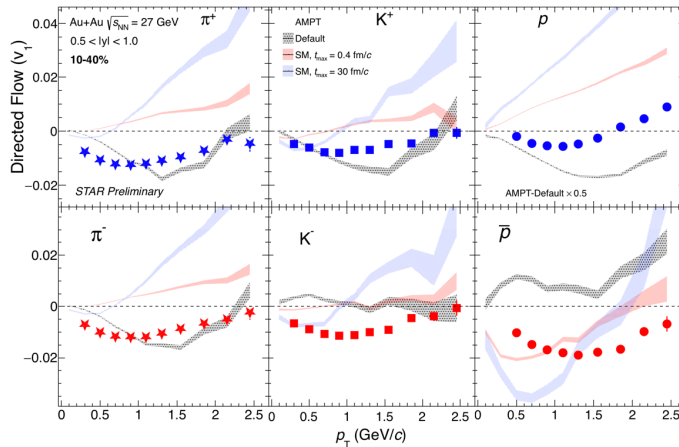


**Fig. 1.**  $v_1$  as a function of  $p_T$  for  $\pi^\pm$ ,  $K^\pm$ ,  $p$  and  $\bar{p}$  in the rapidity region  $0.5 < |y| < 1$  for 10-40% centrality Au+Au collisions at  $\sqrt{s_{NN}} = 27$  GeV. The black, red and blue shaded bands represents AMPT-Default, AMPT-SM with hadronic interaction time  $t_{max} = 0.4$  fm/c and 15 fm/c, respectively [15].

51 Figure 2 shows the  $v_1/n_q$  as a function of  $(m_T - m_0)/n_q$  for  $\pi^+$ ,  $K^+$ ,  $p$   
 52 (upper row) and  $\pi^-$ ,  $K^-$ ,  $\bar{p}$  (lower row) in the rapidity  $0.5 < |y| < 1$  for 10-40%

53 centrality in Au+Au collisions at  $\sqrt{s_{\text{NN}}} = 19.6$  (left panel), 27 (middle panel)  
 54 and 54.4 (right panel) GeV. It is observed that NCQ scaling does not hold well  
 55 for the particles ( $\pi^+$ ,  $K^+$  and  $p$ ) in all the measured energies. The magnitude  
 56 of the violation also increases with decrease in energy as the transported quark  
 57 contribution to the form hadrons increases. However, the NCQ scaling holds  
 58 better for produced hadrons like  $K^-$  and  $\bar{p}$  as these are formed via coalescence  
 59 for quarks and anti-quarks [16].

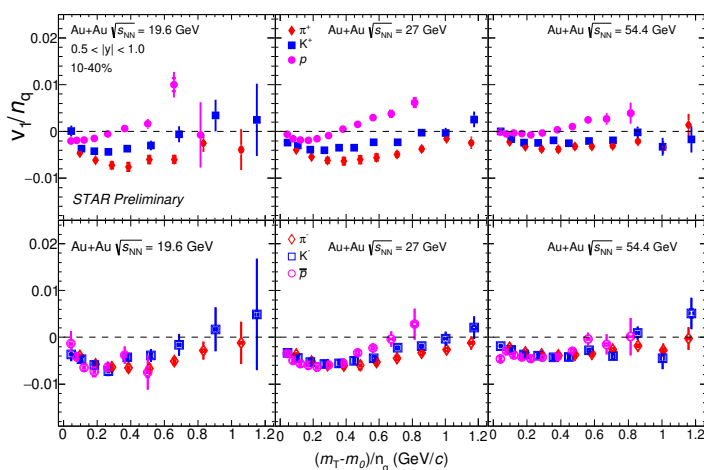


**Fig. 2.**  $v_1/n_q$  vs  $(m_T - m_0)/n_q$  for  $\pi^+$ ,  $K^+$ ,  $p$  (upper row) and  $\pi^-$ ,  $K^-$ ,  $\bar{p}$  (lower row) in the rapidity  $0.5 < |y| < 1$  for 10-40% centrality in Au+Au collisions at  $\sqrt{s_{\text{NN}}} = 19.6, 27$  and  $54.4$  GeV in the left, middle and right column, respectively.

60 Figure 3 shows the centrality dependence of  $v_1/n_q$  as a function of  $(m_T -$   
 61  $m_0)/n_q$  for  $\pi^-$ ,  $K^-$ ,  $\bar{p}$  in 40-80% (left), 10-40% (middle) and 0-10% (right) panel  
 62 in Au+Au collisions at  $\sqrt{s_{\text{NN}}} = 27$  GeV (upper row) and  $54.4$  GeV (lower row).  
 63 The NCQ scaling holds better for produced hadrons such as  $K^-$  and  $\bar{p}$  in all  
 64 three centralities in the low- $m_T$  region.

### 65 3 Conclusion

66 First comprehensive measurements of  $p_T$  dependence directed flow of identified  
 67 hadrons ( $\pi^\pm$ ,  $K^\pm$ ,  $p$  and  $\bar{p}$ ) in the rapidity region of  $0.5 < |y| < 1.0$  for various  
 68 collision centralities in Au+Au at  $\sqrt{s_{\text{NN}}} = 19.6, 27$  and  $54.4$  GeV are reported.  
 69 In the low- $p_T$  region, anti-flow is observed in the measured rapidity region  $0.5$   
 70  $< |y| < 1$  for all hadrons in these energies. The NCQ scaling is observed for  
 71 produced hadrons ( $K^-$  and  $\bar{p}$ ) which suggests that coalescence is the dominant  
 72 mechanism of particle formation for these hadrons. For other hadrons such as  
 73  $\pi^\pm$ ,  $K^+$  and  $p$ , the NCQ scaling is violated as they also receive contribution from

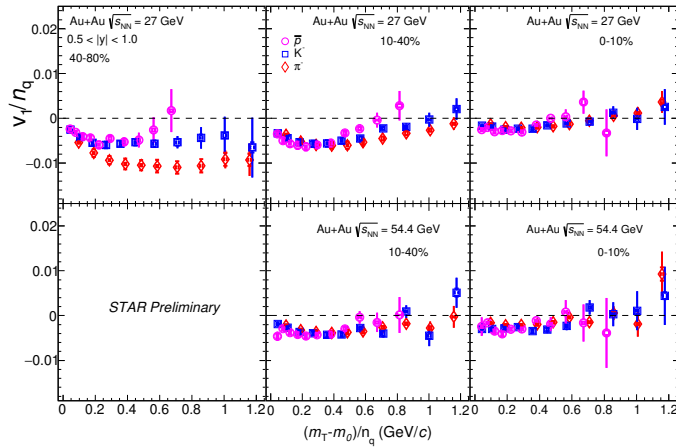


**Fig. 3.**  $m_T$  scaling for  $\pi^-$ ,  $K^-$ ,  $\bar{p}$  in  $0.5 < |y| < 1$  for 40-80% (left), 10-40% (middle) and 0-10% (right) centrality in Au+Au at 27 (upper row) and 54.4 (lower row) GeV.

74 transported quarks along with the primary produced quarks. The contribution of  
 75 transported quarks increases with decrease in energy and hence deviation from  
 76 the NCQ scaling increases.

## 77 4 Acknowledgments

78 This work is supported in part by the National Natural Science Foundation of  
 79 China under Grants No. 11890711, National Key Research and Development  
 80 Program of China under Grant No. 2020YFE0202002 and China Postdoctoral  
 81 Science Foundation under Grant No. 2019M662681.

## 82 References

- 83 1. J. Adams *et al.* (STAR Collaboration); Nucl. Phys. A 757, 102 (2005).
- 84 2. H. Stöcker, Nucl. Phys. A 750, 121 (2005).
- 85 3. C. Zhang *et al.*, Phys. Rev. C 97, 064913 (2018).
- 86 4. Z. Fodor and S. D. Katz, JHEP 0203, 014 (2002); JHEP 0404, 050 (2004).
- 87 5. L. Adamczyk *et al.* (STAR Collaboration), Phys. Rev. Lett. 110, 142301 (2013).
- 88 6. L. Adamczyk *et al.* (STAR Collaboration), Phys. Rev. Lett. 116, 062301 (2016).
- 89 7. S. Shi, Adv. High Energy Phys., 1987432 (2016).
- 90 8. L. Adamczyk *et al.* (STAR Collaboration): Phys. Rev. Lett. 120, 062301 (2018).
- 91 9. E. E. Zabrodin *et al.*, Phys. Rev. C 63, 034902 (2001).
- 92 10. S. A. Voloshin, Nucl. Phys. A 638, 455-458 (1998).
- 93 11. L. V. Bravina *et al.*, Eur. Phys. J. A 52, 245 (2016).
- 94 12. S. A. Voloshin, Phys. Rev. C 55, R1630(R) (1997).
- 95 13. R. J. M. Snellings *et al.*, Phys. Rev. Lett. 84, 2803-2805 (2000).
- 96 14. J. C. Dunlop *et al.*, Phys. Rev. C 84, 044914 (2011).
- 97 15. K. Nayak *et al.* Phys. Rev. C 100, 054903 (2019).
- 98 16. Md. Nasim and S. Singha, Phys. Rev. C 97, 064917 (2018).